Atrial Spiral Wave Drifting Under Applied Spatial Temperature Gradients

Guy Malki, Sharon Zlochiver

Department of Biomedical Engineering, Tel Aviv University, Tel Aviv, Israel

Abstract

Spiral wave drifting and meandering are known measures for cardiac instability and arrhythmogenesis. This study was aimed to analyze spiral wave drifting due to temperature heterogeneity that is applied artificially. Our hypothesis is that spatial temperature gradients (STGs) will cause spatial excitability heterogeneity, which in turn will affect the spiral waves' dynamics. This may help to detect, map and distinguish cardiac spiral waves from ectopic foci, and improve the management of arrhythmias. Cardiac electrical conduction was simulated in 2D tissue models and stable rotors were initiated. The effect of temperature on the rate constants of gating variables was incorporated. When linear STG was applied, spiral waves drifted diagonally towards the colder region of the tissue. We conclude that by artificially employing local temperature heterogeneity, controlled spiral wave can be established allowing potential identifying this arrhythmia driver and tracking its trajectory.

1. Introduction

Cardiac arrhythmias are a major health problem, and atrial fibrillation (AF) is the most common arrhythmia, affecting more than 10% of the population older than 70 years old with an upward trend (1). AF is characterized by rapid and irregular activation of the atrium, approximately 400-600 pulses per minute, and is often the result of fibrillatory conduction maintained by the existence of one or few organized "mother rotors", or alternatively by the existence of focal ectopic source (2,3). AF is traditionally treated using antiarrhythmic rhythm or rate control drugs, that increase the action potential duration (APD) and the refractory period; nonetheless, as pharmacological treatment for AF shows limited success (4), surgical ablation procedures have become attractive in symptomatic patients. These procedures try to isolate arrhythmogenic sources in the atrial tissue and destroy them by ablation. The correct characterization (rotors vs. focal activity) and localization of the arrhythmogenic sources are of crucial importance for a successful outcome of such procedures. However, the existing electrogram-guided source-mapping techniques have not proven to significantly improve the success rate of ablations (4,5). Therefore, there is a clear need for new approaches to correctly and robustly map the arrhythmogenic drivers.

We propose a novel strategy for characterization and localization of specific arrhythmogenic drivers – cardiac rotors (6) – by inducing controlled drifting under spatial temperature gradients (STGs). Rotor drifting and meandering can arise without external intervention, for example due to ion channel gradients (7,8). Existing experimental and numerical evidence suggest that rotor drifting occurs towards low excitability regions (9,10), the origins of which may vary, for instance, spatial heterogeneity in I_{K1} channel distribution (11). Similarly, we postulate that externally applied temperature gradients may establish heterogeneity in atrial excitability, resulting in rotor drifting. It is well known that temperature variations modulate the rate constants of the ion channel gating variables and consequently alter electrophysiological parameters, e.g., action potential morphology and conduction dynamics. Nevertheless, the effects of temperature variations have not yet been studied in detail in the cardiac tissue, possibly due to small physiological variations *in-vivo*. However, large temperature gradients can be artificially introduced and exploited for clinical applications, e.g., to distinguish between rotors that can drift and stable ectopic foci, to track and even control rotor drifting trajectory, and to overall improve the mapping of arrhythmogenic sources during ablation procedures.

2. Methods

2.1. Mathematical model

Cardiac electrical conduction was simulated in 2D tissue models by numerically solving the following reaction-diffusion equation:

$$\frac{\partial V_m}{\partial t} = -\frac{(I_{ion} + I_{stim})}{C_m} + \nabla \cdot (D \nabla V_m) \qquad (1)$$

where V_m [mV] is the transmembrane voltage, C_m [μF/cm^2] is the membrane capacitance per unit area, I_{stim} and I_{ion} [μA/cm^2] are the external stimulation and

membrane ionic currents, respectively, and D [mm^2/ms] is the diffusion coefficient. Human atrial kinetics were employed for calculating I_{ion} using the Courtemanche-Ramirez-Nattel (CRN) model (12). This model consists of 12 ionic currents, which are based on recorded data from human atrial myocytes, along with representations of pumps, exchangers and background currents. The model was modified to incorporate chronic AF remodeling (9,13) by down-regulating the densities of the transient outward K+ current, I_{to} (by 50%), the ultra-rapid delayed rectifier K+ current, I_{Kur} (by 50%), the L-type Ca2+ current, I_{CaL} (by 70%), and by increasing in the density of the inward rectifier K+ current, I_{K1} (by 100%). The effect of temperature on the model dynamics was incorporated by multiplying the various channel gating rate constants (α, β) (or alternatively by dividing the channel time constants(τ)) by the temperature adjustment factor Q(T),

$$Q(T) = Q_{10}^{\frac{T-T_0}{10℃}} = Q_{10}^{\frac{T-37℃}{10℃}} \quad (2)$$

$$\tau(T) = \frac{1}{\alpha(T)+\beta(T)} = \frac{\tau(37°C)}{Q(T)} \quad (3)$$

where T [℃] is the local tissue temperature, T_0 is the reference temperature (normally set to 37°C) and Q_{10} is the ratio by which the rate constants increase following a temperature increment of 10°C. Q_{10} factors for the gating variables for I_{Na}, I_{CaL}, I_{to}, I_{kur}, I_{kr} and I_{ks} currents were taken from the literature, as detailed in Table 1.

Table 1. Q_{10} values for each ionic current.

Current	Q_{10}	Reference
I_{Na}	3	(Sakakibara et al. 1992)
I_{to}	2.2	(Wang et al. 1993)
I_{Kur}	2.2	(Wang et al. 1993)
I_{kr}	3.3	(Mazhari et al. 2001)
I_{ks}	2.57	(Terrenoire et al. 2005)
$I_{Ca/L}$	2.2	(ten Tusscher et al. 2004)

It should be noted that temperature changes also influence the Nernst potentials for the various ions, and had been taken into account. However, this effect is in a much lesser extent.

2.2. Computational simulations

Equation (1) was numerically solved using the finite-difference method in combination with Euler integration in time. Coding was performed using the C++ MPI library on a cluster computer. MATLAB was used for data analysis and visualization. Single cell simulations were conducted to characterize basic mechanisms and electrophysiological effects of temperature changes on the cardiac myocyte electrodynamics, e.g., APD, tissue excitability and the various ion channels characteristics. 2D simulations were performed on square atrial tissue with an area of 900mm^2, with spatial and temporal resolution of Δh=0.1mm and Δt=0.0025ms, respectively. Isotropic diffusion coefficient of D=0.03 mm^2/s was set, resulting in a physiological planar conduction velocity of about 0.3 m/s. Initial conditions were taken similar to those described in (12).

STGs were achieved by employing a linear temperature gradients along the y-axis between a reference body temperature of T_1=37°C and varying T_2 as can be seen in Figure 1. Spiral waves were established approximately in the middle of the tissue using standard cross-field stimulation, and were stable prior to the application of the STG.

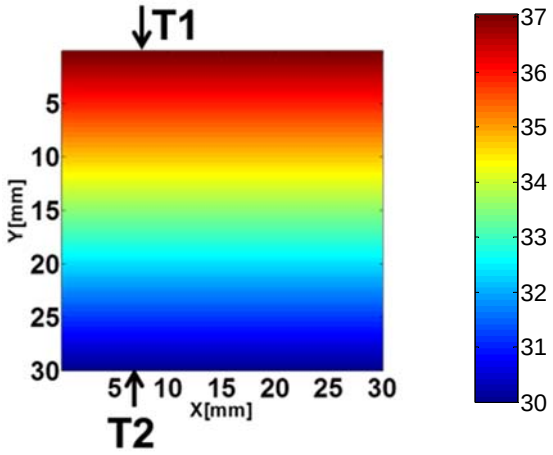

Figure 1. STGs patterns: Linear temperature gradient between T_1=37°C and T_2=30°C (left) and local circular temperature perturbation with radius of 2mm (right).

2.3. Data analysis

Spiral tip trajectory was calculated and was plotted for each simulation. The spiral tip location was calculated as the point of intersection of the -15mV iso-potential line and the line $\frac{dV_m}{dt} \approx 0$. Ion channel state variables were recorded during the entire simulation duration. Spatial excitability distribution in each configuration was estimated by calculating sodium channel availability, i.e., the product of the fast (*h*) and slow (*j*) inactivation state variables.

3. Results and discussion

3.1. Single cell

The effect of temperature on action potentials (APs)

and on sodium channel availability is shown in Figure 2 for both the original CRN and the modified chronic AF models. The results demonstrate that in both models, recovery time increased as the temperature decreased, i.e., excitability became lower. This is due to the decreased rates of gating dynamics in colder temperatures. The effect of temperature on the AP morphology was substantial in the original CRN model, with decreasing temperatures resulting in significant prolongation of the AP duration. In contrast, the effect of temperature in the chronic AF model was minor, but still there was a clear difference between the sodium availability at specific time-point at each temperature.

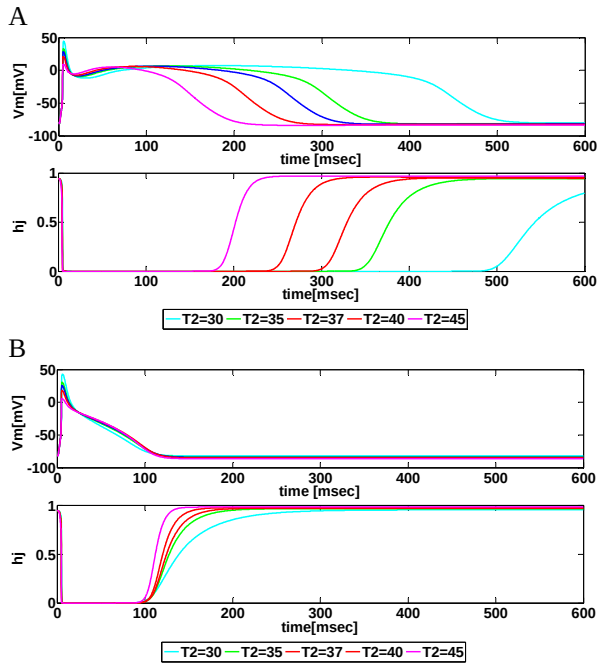

Figure 2. Single cell atrial action potentials and sodium channel availability using the CRN model (A) and chronic AF modifications (B).

3.2. 2D models

Linear STGs were first applied with a reference temperature of $T_1 = 37℃$ at the upper edge of the tissue, and a varying T_2 between 30℃ to 45℃ at the bottom edge. A typical case is shown in Figure 3, where the top panel displays several snapshots of V_m at t=500, 2500 and 4500 msec post STG activation, for the specific case of $T_2 = 30℃$. The bottom panel presents the spatial distribution of the maximum value of the *hj* product corresponding to the same activation cycle that is associated with the displayed snapshots.

As can be seen, the spiral wave drifted towards the colder region in a diagonal trajectory to the bottom-left corner. The vertical drift was due to the heterogeneity in tissue excitability, towards the less excitable region, as demonstrated in the bottom panel, while the horizontal drift was due to the anti-clockwise chirality of the rotating wave.

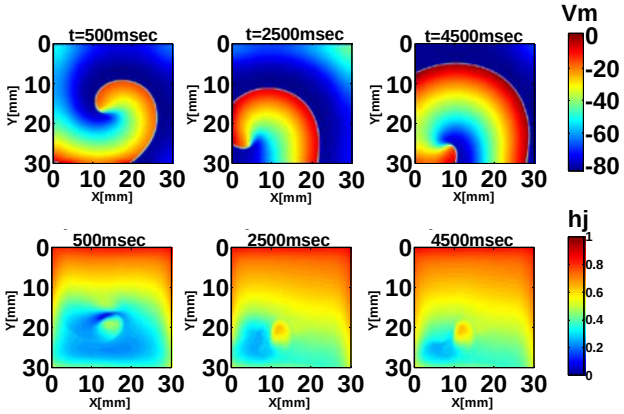

Figure 3. Transmembrane voltage snapshots (top) and maximal sodium channel availability (bottom) for a linear STG with T_2=30°C.

This result is consistent with previous studies linking rotor drifts towards regions with prolonged action potential durations or reduced excitability (11,14). This result was consistent for all other values of T_2, as shown in figure 4, illustrating the tip trajectory as a function of both time (z-axis) and space. The mean route of the spiral wave core center was also calculated and plotted in bold lines. In all cases, the spiral wave drifted towards the colder region of the tissue, with the maximal drifting translation distance depending on the gradient magnitude. With larger temperature gradients, the drifting occurred with higher velocity and larger translation distance.

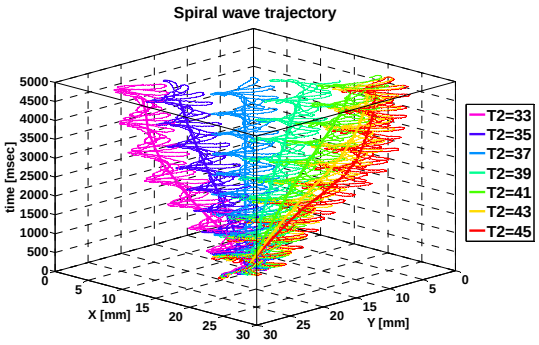

Figure 4. Spiral wave spatiotemporal trajectories for linear STGs of varying T_2.

4. Conclusions

The presented simulations demonstrate that tissue temperature heterogeneity causes predictable spiral wave drifting due to the manifestation of excitability heterogeneity. Hence, local temperature perturbation may be potentially employed in prospective clinical devices to [detect and characterize rotor drifting and trajectory, aiding in procedures such as atrial ablations. Further work is needed to address the inverse problem of reconstructing rotor trajectories in the tissue under prescribed STGs.

Acknowledgements

This work was supported in part by a grant from the Nicholas and Elizabeth Slezak Super Center for Cardiac Research and Biomedical Engineering at Tel Aviv University.

References

[1] Nattel S. New ideas about atrial fibrillation 50 years on. Nature 2002;415(6868):219–26.

[2] Pandit SV, Jalife J. Rotors and the dynamics of cardiac fibrillation. Circ Res 2013;112:849–62.

[3] Baher A, Qu Z, Hayatdavoudi A, Lamp ST, Yang M-J, Xie F, et al. Short-term cardiac memory and mother rotor fibrillation. Am J Physiol Hear Circ Physiol 2007; 292:H180–9.

[4] Nattel S. Experimental evidence for proarrhythmic mechanisms of antiarrhythmic drugs. Cardiovasc Res 1998;37:567–77.

[5] Kang Teng L, Sébastien K, Matthew W, Michel H. Atrial substrate ablation in atrial fibrillation. In: Jalife J, Zipes DP, editors. Cardiac Electrophysiology, from cell to bedside. 2009. p. 1059.

[6] Comtois P, Kneller J, Nattel S. Of circles and spirals: bridging the gap between the leading circle and spiral wave concepts of cardiac reentry. Europace 2005;7:10–20.

[7] Ten Tusscher KHWJ, Panfilov AV. Reentry in heterogeneous cardiac tissue described by the Luo-Rudy ventricular action potential model. Am J Physiol Heart Circ Physiol 2003;284:H542–8.

8]Xie F, Qu Z. Electrophysiological heterogeneity and stability of reentry in simulated cardiac tissue. Am J Physiol Hear Circ Physiol 2001;280:535–45.

[9] Pandit SV, Berenfeld O, Anumonwo JMB, Zaritski RM, Kneller J, Nattel S, et al. Ionic determinants of functional reentry in a 2-D model of human atrial cells during simulated chronic atrial fibrillation. Biophys J. 2005;88:3806–21.

[10]Jalife J, Gray R. Drifting vortices of electrical waves underlie ventricular fibrillation in the rabbit heart. Acta Physiol Scand 1996;157:123–31.

[11]Calvo CJ, Deo M, Zlochiver S, Millet J, Berenfeld O. Attraction of rotors to the pulmonary veins in paroxysmal atrial fibrillation: A modeling study. Accept Publ Biophys J 2014.

[12]Courtemanche M, Ramirez RJ, Nattel S. Ionic mechanisms underlying human atrial action potential properties: insights from a mathematical model. Am J Physiol Hear Circ Physiol. Am Physiological Soc 1998;275(1 Pt 2):H301–H321.

[13]Courtemanche M, Ramirez RJ, Nattel S. Ionic targets for drug therapy and atrial fibrillation-induced electrical remodeling: insights from a mathematical model. Cardiovasc Res 1999;42:477–89.

[14]Pertsov a. M, Davidenko JM, Salomonsz R, Baxter WT, Jalife J. Spiral waves of excitation underlie reentrant activity in isolated cardiac muscle. Circ Res 1993;72:631–50.

Address for correspondence:

Guy Malki
Biomedical Engineering Dept., Tel Aviv University, 6997801, Tel-Aviv, Israel.
guymalki@gmail.com